Magnetization transfer imaging of the head and neck: normative data.

D M Yousem, M D Schnall, L Dougherty, G S Weinstein and R E Hayden

AJNR Am J Neuroradiol 1994, 15 (6) 1117-1121
http://www.ajnr.org/content/15/6/1117

Magnetization Transfer Imaging of the Head and Neck: Normative Data

David M. Yousem, Mitchell D. Schnall, Lawrence Dougherty, Gregory S. Weinstein, and Richard E. Hayden

PURPOSE: To determine magnetization transfer ratios for normal head and neck structures so that evaluation of disease will be possible. **METHODS:** Two-dimensional magnetization transfer imaging was performed in 12 healthy volunteers and 20 patients. We used a repetition time of 500, echo time of 12, 20° flip angle, and a magnetization transfer pulse offset from the resonance frequency of water by 2000 Hz (pulse duration 19 milliseconds, waveform area approximately 10 times greater than that of a 90° pulse). Magnetization transfer ratios (1 − [intensity after suppression/intensity before suppression]) were calculated for normal structures. **RESULTS:** The magnetization transfer ratio of facial muscles (0.54) was equivalent to that of tongue muscles (0.54). These values exceeded those of parotid (0.39) and submandibular glands (0.41). Fat (0.07) and cerebrospinal fluid (0.05) had negligible transfer. **CONCLUSION:** Magnetization transfer imaging is a simple and effective means of studying the contribution of macromolecular protons to the MR image. Normal neck structures show a wide range of magnetization transfer rates, maximal for muscle and minimal for cerebrospinal fluid and fat.

Index terms: Head, magnetic resonance; Neck, magnetic resonance; Magnetic resonance, technique; Magnetic resonance, tissue characterization

AJNR Am J Neuroradiol 15:1117–1121, Jun 1994

Proton magnetic resonance (MR) is dominated by the contribution of freely mobile water protons because of their great abundance and their sharp resonance frequency. Nevertheless, relaxation of water protons by interactions with macromolecular protons found in proteins and cellular membranes *does* contribute to the signal derived in proton MR. The protons in the macromolecular proteins have restricted motion, and they interact with mobile water protons through dipolar coupling and chemical exchange (1–3).

The macromolecular proton pool appears as a very broad peak in the MR spectrum, extending over approximately 20 kHz. By placing a suppressor pulse far away from the resonant frequency of water into this broad macromolecular pool, one can assess the contribution of the macromolecular protons to the MR signal. This is most easily done by comparing scans with and without the suppressor pulse applied and/or by performing subtraction imaging of these two sequences.

Magnetization transfer imaging (MTI) has been used in research institutions to evaluate lesions of the brain (4–8), liver (9), knee (10), and heart (11). Because the head and neck region contains structures with a wide range of protein, fat, and water content, the implementation of MTI in the head and neck would seem to have great potential. Additionally, because one of the drawbacks of spin-echo MR scanning of the head and neck is the inability to distinguish tumoral edema from tumor cells, MTI ultimately may be useful in defining boundaries of rapidly proliferating cancers. One would expect that differentiation of freely mobile edema protons could be distinguished from the more restricted tumor cell membrane proton pool.

In an attempt to determine the feasibility of MTI in the head and neck, we studied 12 healthy

Received May 26, 1993; accepted after revision September 7.

Presented at the American Society of Head and Neck Radiology course, May 16, 1993.

From the Departments of Radiology and Otorhinolaryngology (D.M.Y., M.D.S., L.D.) and Head and Neck Surgery (D.M.Y., G.S.W., R.E.H.), Hospital of the University of Pennsylvania, Philadelphia.

Address reprint requests to David M. Yousem, MD, Department of Radiology, Hospital of the University of Pennsylvania, 3400 Spruce St, Philadelphia, PA 19104.

AJNR 15:1117–1121, Jun 1994 0195-6108/94/1506–1117

volunteers and 20 consecutive patients to provide normative data for head and neck structures. We sought to assess the intersubject and intrasubject variability of magnetization transfer in normal structures of the head and neck. Ultimately, these baseline data points will be used to contrast with those of head and neck lesions.

Materials and Methods

Twelve healthy volunteers (staff, residents, and fellows of the Department of Radiology at the Hospital of the University of Pennsylvania) without known head and neck disease were recruited for normative MTI data accumulation. All subjects were required to complete informed consent documents, and the study was approved by the Institutional Review Board at the University of Pennsylvania. After the safety and feasibility of the technique in the 12 volunteers were shown to be acceptable, 20 consecutive patients referred to the MR Imaging Center at the University of Pennsylvania for head and neck evaluation also had MTI pulse sequences as part of their scanning protocols. None of the anatomic regions used for accumulation of normative data in these patients had abnormalities, and no patient had been previously treated with either radiation or chemotherapy for head and neck lesions. The age range for the 2 groups of patients was 28 to 72 years.

The MTI scanning protocol used a repetition time of 500 msec, an echo time of 12 msec, and a flip angle of 20° using a multiplanar gradient-echo pulse sequence in a two-dimensional mode. Scanning was performed with and without the magnetization transfer pulse using the same scanning, receive-attenuation, and transmit-attenuation parameters. The magnetization transfer pulse had a duration of 19 milliseconds, was offset from the resonance frequency of water by 2000 Hz, and used an area of waveform approximately 10 times greater than that of the 90° spin-echo pulse. The technique used a single-cycle sinc pulse (typical section selection pulses are 4 cycles) to induce a broad homogeneous suppression without peaks and valleys of side lobes. This suppression pulse is applied approximately 1 millisecond before routine imaging pulses.

The matrix size was 256 × 128, and the section thickness was 5 mm with a 2.5-mm intersection gap. Overall scan time was 2 minutes 10 seconds with and without the MTI pulse applied.

Previous studies using this technique have demonstrated specific absorption rates from 1.16 to 2.89 W/kg for patients with weights between 45 and 136 kg. The average B1 intensity is 3.67×10^{-6} T (9).

The sections through the patients' anatomy were selected to extend from the parotid gland to the infrahyoid neck in the 12 volunteers. In the patients, scans were centered at areas of abnormality but included normal structures for analysis. The anatomy covered and section locations were identical for the pre- and post-MTI suppression scans.

All scans were performed on a 1.5-T General Electric Medical Systems (Milwaukee, Wis) MRI Signa scanner. A Medical Advances (Milwaukee, Wis) volume neck coil was used in each case.

Regions of interest for signal intensity measurements were sampled at the same locations for the scans before and after the magnetization transfer pulse was applied. This was achieved by keeping the position, shape, and volume of the cursor for the region of interest constant between measurements of the pre- and post-MTI sequence. Minor adjustments for patient motion were rarely required. The region of interest sampled was a 4-mm^2 circle. This allowed calculation of the ratio of intensity after suppression to the intensity before suppression. The magnetization transfer ratio (MTR) was defined as 1 − (intensity after suppression/intensity before suppression). By defining the MTR as such, the higher the number the greater the degree of transfer of relaxation. These values (with standard deviations) were obtained for various structures in the head and neck. Right and left asymmetry between the same structures within an individual subject provided intrasubject variability. Intersubject variability was reflected by standard deviations of MTR means for the 32 individuals.

Using the Command Language Image Processing System menu of the General Electric Signa scanner, subtraction images of the two sequences could be obtained. By subtracting the image after suppression from the image before suppression, one could obtain a magnetization transfer image in which higher signal intensity reflected greater magnetization transfer.

The regions of interest that were sampled included the masseter muscles, the pterygoid muscles, the tongue intrinsic muscles, the submandibular glands, the parotid glands, the cerebrospinal fluid (CSF) within the cervical spinal canal, and the subcutaneous fat. The number of entries for different structures varied slightly, because some scans did not encompass all anatomic regions (ie, thyroid glands), or because the 20 patients' disease encompassed regions that would normally have been measured. This, plus the random selection of anatomy to determine right-to-left asymmetry, accounts for the nonuniformity of measurements.

The data were analyzed using the Student's two-tailed *t* test for paired samples. Cases in which two anatomic regions were not examined in a single patient were discarded when looking at pairs of data.

Results

Volunteers and patients showed no adverse reactions to scanning with the magnetization transfer pulse used. It was noted that mild heating was produced by the body coil transmitted to the shoulder regions, but the body and surface coils were never warm to the touch. No danger was posed to a patient or volunteer, even those weighing more than 250 lb.

The MTRs of the masseter and pterygoid muscles were similar and are grouped together in the Table for the determination of muscle MTRs. The Table shows the ratios of the other normal structures of the head and neck.

As expected, CSF and fat, with a predominance of mobile protons, had the lowest MTRs. Muscle, on the other hand, had the highest MTRs, reflective of the greater number of restricted macromolecular protons. The MTR values of the masseter and pterygoid muscle were similar to the value for tongue musculature. Glandular tissue (salivary and thyroid glands) had intermediate values (Fig 1).

Of note was the fairly wide range of standard deviations in the values of the MTRs. In the parotid gland and thyroid glands, this may result from the variable degree of fatty replacement and active glandular tissue, respectively. However, similar standard deviations were noted in all head and neck structures.

When the right and left sides were compared in the evaluation of muscles or glands, the mean MTR variation was 0.11 with an SD of 0.10. To an extent this may reflect inhomogeneities in the magnetic field, surface coil asymmetric placement, or the natural limitation of the MTI technique. These data alternatively may reflect intrasubject variability. There was no consistent pattern for the right-to-left asymmetry, and variability was found in all measured structures, including muscles, glands, and tonsils.

Using the Student's *t* test, there was a statistically significant difference ($P < .01$) in MTR values between muscle and the submandibular gland, parotid gland, CSF, and fat, but not for tongue, tonsils, or thyroid tissue (the latter possibly attributable to the small sample size of just 17 pairs of data). A statistically significant difference ($P < .01$) in MTR values between the submandibular gland and tongue, tonsil, CSF, and fat was noted but not between the submandibular gland and parotid or thyroid glands. Similarly, the parotid gland's MTR and all other structures' MTRs except the thyroid gland and tonsil were different with statistical significance. The MTRs of CSF and fat differed from those of all other structures except each other. The thyroid gland and tonsil MTR values did not differ significantly.

Normal structures and MTRs

Structure	Number of Measurements	Mean MTR	SD
Muscle (pterygoid, masseter)	100	0.54	0.09
Submandibular gland	41	0.41	0.09
Parotid gland	50	0.39	0.09
Tongue (genioglossus)	32	0.54	0.11
CSF	46	0.05	0.03
Fat	32	0.07	0.04
Thyroid	17	0.41	0.15
Tonsil	37	0.44	0.09

Discussion

Although in many cases MR has improved on computed tomography in the evaluation of head and neck lesions, the boundaries of neoplasms from adjacent normal structures may sometimes be indistinct in all cross-sectional imaging modalities. Computed tomography is limited to the evaluation of x-ray beam attenuation and iodine enhancement in its contrast determination, but MR is more diverse in the types of contrast obtainable: T1 weighting, proton-density weighting, T2 weighting, contrast enhancement, flow, and response to gradient echoes. Nonetheless, MR continues to be limited in the head and neck (as elsewhere) in distinguishing tumor from peritumoral edema. Additionally, histologic discrimination in distinguishing benign from malignant neoplasms and inflammatory from neoplastic processes continues to be elusive. Because of these shortcomings, it is useful to evaluate new MR imaging techniques for improvements to current pulse sequences.

MTI is a method of determining the contribution of macromolecular protein and cell wall protons to the MR signal. One would expect that highly cellular or proteinaceous lesions would provide greater magnetization transfer. Neoplasms, because of cellular proliferation, should have greater magnetization transfer than that of inflammatory lesions or edema, which are dominated by increased free water protons. A hypothetical goal of head and neck MTI would be to distinguish edema from normal tissue from cancer by virtue of the relative contributions of macromolecular protein cross-relaxation (magnetization transfer) to signal intensity. Iwama et al have shown that cross-relaxation decreases significantly in peritumoral edematous rat brains compared with normal rat brains (12). The astrocytic tumors themselves had a slight increase in cross-relaxation compared with normal brain tissue. Boorstein et al also have shown that MTRs are decreased in the white matter surrounding

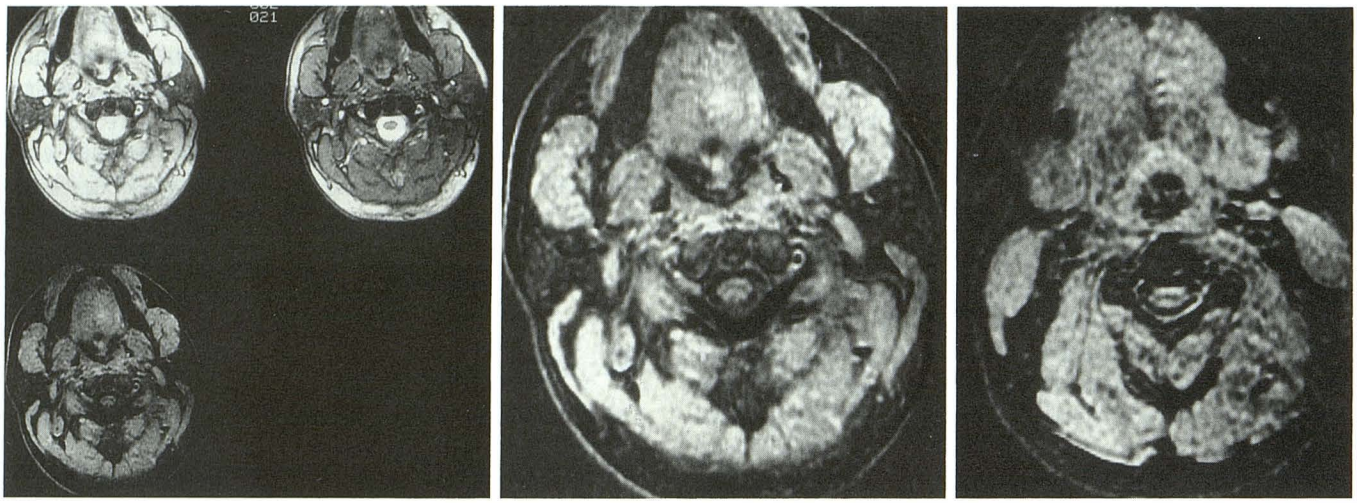

Fig. 1. Healthy volunteer with source images, MTI subtraction images.

A, Scan through the parotid gland level with multiplanar gradient-echo technique before magnetization transfer pulse was applied (*upper left*), after magnetization transfer pulse applied (*upper right*), and subtraction image (before minus after) (*bottom right*). Compare intensities of various tissues, and note greatest change in muscle.

B, Magnified subtraction image of scan before MTI minus scan after MTI provides an image on which the degree of change is reflected in signal intensity. CSF, fat, and fatty parotid have low intensity because little change (magnetization transfer) has occurred. Muscle is brighter because there has been more transfer.

C, A subtracted image through the submandibular glands shows intermediate intensity (transfer) compared with muscle and CSF. Note the asymmetry from right to left, possibly caused by inhomogeneity in field.

metastatic lesions in the human brain, both in areas of bright signal on T2-weighted sequences and in areas that appeared normal on all spin-echo images (8). They propose that MTI ultimately may help in mapping tumors for radiation therapists. The utility of the technique in the head and neck must be examined.

Lundbom has examined the role of MTI in determining the histologic grade of brain tumors (7). The mean MTR of high-grade astrocytomas was greater than that of low-grade astrocytomas ($P = .0005$), presumably because of a difference in cellularity and nuclear material. The MTRs of astrocytomas were significantly smaller than those of meningiomas and pituitary adenomas. Applied to the head and neck, MTI may prove useful in predicting histologic grades of squamous cell carcinoma because well-differentiated tumors have more keratin and are less cellular (a lower MTR), whereas poorly differentiated carcinomas should have more nuclear material (higher MTR). Will MTI aid in distinguishing lymphomas from squamous cell carcinomas, reactive lymphadenopathy from malignant nodes? Research in these areas may prove fruitful.

In this preliminary study we have explored MTRs of nondiseased anatomic structures of the head and neck to provide normative data. By providing early baseline values, as well as a protocol for an easily implemented MTI technique, we hope to encourage a uniform approach to the evaluation of this technique. Comparing techniques with varying scan parameters makes the overall evaluation of a sequence much more difficult. We advocate adopting a standardized, universal approach to MTI of the head and neck using the parameters provided herein. We hope that the scan technique provided here will allow head and neck investigators to define more readily the role of MTI in the head and neck.

It is gratifying when the theoretical expectations of a technique are substantiated with clinical implementation. One would expect that muscle, because of the high macromolecular protein proton content, would have the highest MTR. This is in fact what was demonstrated here. In a similar vein, CSF, with an absence of macromolecular proteins, would be expected to have negligible transfer, as demonstrated. A small amount of suppression of water by the broad magnetization transfer suppressor pulse may explain why the MTR values are not absolute zero for water. Fat, also dominated by highly mobile protons without protein contributions, also showed very low MTRs. The submandibular and parotid glands have a variable contribution of fat, glandular

elements, and secretions. The intermediate transfer ratios in these structures are therefore not fully unexpected.

Although the intrasubject variabilities from right to left and intersubject variability in MTRs was moderately large, we do not believe that these ranges will obviate the application of the technique for the evaluation of pathologic conditions of the head and neck. As coil design allows more and more homogeneous fields, and more age- and sex-matched subjects are accrued in the MTI data base, we expect these asymmetries and variabilities to decline. At this time we have no definite explanation for the variability, nor any further suggestions for improving the homogeneity of values.

Previous investigators have reported magnetization transfer results in terms of intensities before and after suppression pulses. By using 1 minus this ratio, the higher number will reflect the greater transfer. Converting prior studies' results into our nomenclature shows remarkable similarity with muscle MTRs ranging from 0.49 to 0.60 (9, 11, 13), fat from 0.0 to 0.05 (1, 9), and CSF 0.0 to 0.07 (1, 6, 7, 9). Standard deviations of means reported in these studies are also similar to our results. These values are remarkably consistent considering that the field strengths, scanning parameters, locations of structures, and even species varied from our study.

Armed with normative data and a user-friendly MTI pulse sequence, one is now prepared to evaluate the applications of the technique in pathologic conditions. We predict that the differentiation of inflammatory and neoplastic lesions, hypercellular and hypocellular masses, and edema versus neoplasms will be distinguishable by MTI in the head and neck. One would hope that creating subtraction images, which currently requires entering the scanner's software programs, will become easier as the utility of the technique is borne out.

References

1. Wolff SD, Balaban RS. Magnetization transfer contrast (MTC) and tissue water proton relaxation *in vivo*. *Magn Reson Med* 1989;10:135–144
2. Eng J, Ceckler TL, Balaban RS. Quantitative ^{1}H magnetization transfer imaging *in vivo*. *Magn Reson Med* 1991;17:304–314
3. Fralix TA, Ceckler TL, Wolff SD, Simon SA, Balaban RS. Lipid bilayer and water proton magnetization transfer: effect of cholesterol. *Magn Reson Med* 1991;18:214–223
4. Wolff SD, Eng J, Balaban RS. Magnetization transfer contrast: method for improving contrast in gradient-recalled-echo images. *Radiology* 1991;179:133–137
5. Lipton MJ, Sepponen RE, Tanttu JI, Kuusela T. Magnetization transfer technique for improved magnetic resonance imaging contrast enhancement in whole body imaging. *Invest Radiol* 1991;26:S255–S256
6. Dousset V, Grossman RI, Ramer KN, et al. Experimental allergic encephalomyelitis and multiple sclerosis: lesion characterization with magnetization transfer imaging. *Radiology* 1992;182:483–491
7. Lundbom N. Determination of magnetization transfer contrast in tissue: an MR imaging study of brain tumors. *AJR Am J Roentgenol* 1992;159:1279–1285
8. Boorstein JM, Grossman RI, Bolinger L. Magnetization transfer imaging in metastatic disease to the brain. *Radiology* (in press)
9. Outwater E, Schnall MD, Braitman LE, Dinsmore BJ, Kressel HY. Magnetization transfer of hepatic lesions: evaluation of a novel contrast technique in the abdomen. *Radiology* 1992;182:535–540
10. Wolff SD, Chesnick S, Frank JA, Lim KO, Balaban RS. Magnetization transfer contrast: MR imaging of the knee. *Radiology* 1991;179:623–628
11. Balaban RS, Chesnick S, Hedges K, Samaha F, Heineman FW. Magnetization transfer contrast in MR imaging of the heart. *Radiology* 1991;180:671–675
12. Iwama T, Yamada H, Era S, et al. Proton nuclear magnetic resonance studies on water structure in peritumoral edematous brain tissue. *Magn Reson Med* 1992;24:53–63
13. Tanttu JI, Kahn CE Jr, Sepponen RE, et al. Magnetization transfer contrast of body tissues in vivo in MR imaging (abstr). *Radiology* 1990;177(P):245